

# Control Strategy and Characteristic Analysis of Hybrid Active Power Filters with the Resonant Impedance Principle

Lu Fang<sup>†\*</sup>, Xian-yong Xu<sup>\*\*</sup>, An Luo<sup>\*</sup>, Yan Li<sup>\*</sup>, Chun-ming Tu<sup>\*</sup>, and Hou-hui Fang<sup>\*</sup>

<sup>†\*</sup>College of Electrical and Information Engineering, Hunan University, Changsha, China

<sup>\*\*</sup>Hunan Electric Power Company Test and Research Institute, Hunan Electric Power Company, Changsha, China

## Abstract

A new kind of resonant impedance type hybrid active filter (RITHAF) is proposed for dynamic harmonic current suppression and high capacity reactive compensation in medium and high voltage systems. This paper analyzed the different performance of the RITHAF when the active part of the RITHAF is controlled as a current source and as a voltage source, respectively. The harmonic suppression function is defined in this paper. The influences of the changes caused by the grid impedance and the detuning of the passive power filter on the compensating characteristics of the RITHAF are studied by analyzing the suppression function. Simulation and industrial application results show that the RITHAF has excellent performances in harmonic suppression and reactive compensation, which is suitable for medium and high voltage systems.

**Key words:** Compensation Characteristics, Control Strategy, Harmonic Suppression, Harmonic Suppression Function, Hybrid Active Power Filter, Reactive Compensation

## I. INTRODUCTION

Due to the wide application of power electronic loads such as switching mode power supplies, light controllers, interruptible power supplies, electric furnaces, ac voltage regulators and adjustable speed drives, a large amount of harmonic current or voltage is produced and reflected into distribution and transmission networks, which degrades the power quality [1], [2]. In order to mitigate harmonics, different configurations of active and passive filters have been proposed for different applications.

Conventionally, passive power filters (PPF) are often used to improve power quality due to its simple circuit configuration. Bulky passive elements, fixed compensation characteristics, and series and parallel resonance are the main drawbacks of this scheme. To overcome such problems, active power filters (APF) have been used effectively since they can compensate

harmonics dynamically. The shunt connection APF is the most studied topology [3]-[7]. However, these APF are not suitable for high or medium voltage situations because the capacity of semiconductor components is not high. In order to reduce the capacity of power devices, hybrid compensation schemes have emerged one after another. The aim of hybrid topologies is to enhance passive filter performance and to reduce the power-rating of active filters [8]-[15]. A shunt active power filter applied to high-voltage power distribution systems has been presented [12]. This system was based on the transformer's harmonic impedance control. Active power filters naturally provides a low impedance path for harmonic currents in power systems. The harmonic currents in power distribution systems can be led to flow into the linear transformer branch. A combined system of a classical static var compensator (SVC) and an APF has been proposed [13]. The SVC in this system consists of a PPF and a thyristor controlled reactor (TCR). A small rating APF was used to improve the filtering characteristics of the PPF and to suppress the possibility of resonance between the grid and the PPF. A novel three-phase hybrid active power filter with a series resonance circuit tuned at the fundamental frequency was proposed for simultaneously suppressing harmonic currents and compensating high-capacity reactive power in high- and

Manuscript received Feb. 12, 2012; revised Oct. 7, 2012

Recommended for publication by Associate Editor Sanjib Kumar Panda.

<sup>†</sup>Corresponding Author: 2001xxy@163.com

Tel: +86-731-88823964, Hunan University

<sup>\*</sup>College of Electrical and Information Eng., Hunan University, China

<sup>\*\*</sup>Hunan Electric Power Company Test and Research Institute, Hunan Electric Power Company, China

medium-voltage power systems [14]. The active power filter was shunted to the series resonance circuit by a matching transformer which greatly reduces its current requirements as well as the voltage ratings of the semiconductor switching devices. Passive power filters were used to compensate reactive power with a constant capacity. The active part in [13], [14] was a hybrid active power filter with an injection circuit (IHAPF), which showed great promise in reducing harmonics and improving the power factor with a relatively low capacity active power filter. However, it suffered from dc-side voltage instability that inadvertently impacted the compensation performance and the safety of the IHAPF. Two new methods were proposed to overcome this major technical challenge. One uses a hysteretic control and energy release circuit, and the other uses a controllable pulse width modulation (PWM) rectifier [15].

A new kind of Resonant Impedance Type Hybrid Active Filter (RITHAF) is proposed in this paper. The topology and operation principle of the RITHAF are described in Section II. The work characteristic is analyzed when the RITHAF is controlled as current source and as a voltage source in Section III. The compensation characteristics of the RITHAF, the influence of system parameters changes and Passive Power Filter Detuning are analyzed in Section IV. In Section V and VI simulation and industrial application results demonstrate that the proposed RITHAF can effectively suppress harmonics and compensate reactive power, while using economic, low capacity APFs. Finally, some conclusions have been given in Section VII.

## II. SYSTEM CONFIGURATION AND WORKING PRINCIPLE OF THE RITHAF

### A. Topology of the RITHAF

The structure of the RITHAF is shown in Fig.1. A Voltage Source Converter (VSC) is the active part. The passive part is composed of several single tuned filters and a second order high pass filter. The active part in parallel with a fundamental series resonance circuit (FSRC) through a coupling transformer is connected with the passive section in series. The RITHAF connects to the grid in parallel through its passive part. The VSC is a pulse width modulation inverter based on self-turn-off devices. The DC-side is a capacitor with a high capacity. An output filter is connected with the output of the VSC to filter high order frequency currents. In this structure, the FSRC is connected at the second side of the coupling transformer in parallel. As a result, the RITHAF can compensate a great deal of reactive power with the lower capacity of the VSC. The operation characteristic of the RITHAF is that the reactive power is compensated only by the passive part and the harmonic content is eliminated by both the active and passive parts.

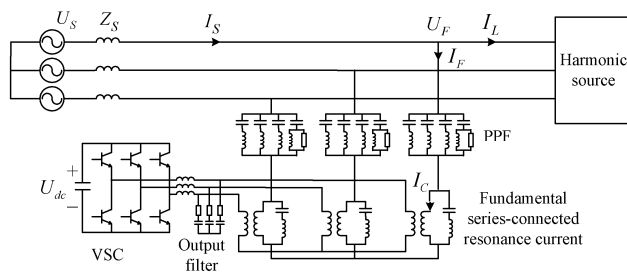


Fig. 1. Configuration of RITHAF.

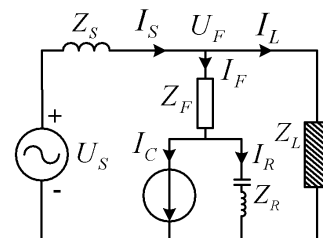


Fig. 2. Single-phase equivalent circuit of RITHAF.

### B. The Basic Working Principle of the RITHAF

The single-phase equivalent circuit of the RITHAF is shown in Fig.2. The nonlinear load  $Z_L$  is viewed as a harmonic source. It is a harmonic current source  $I_{Lh}$  if only the harmonic components of the system are considered. It is the fundamental wave impedance  $Z_{Lf}$  if only the fundamental component of the system is considered.  $U_S$  is the voltage of the grid. The active part is given as a controlled current source.  $I_S$ ,  $I_L$ ,  $I_F$ ,  $I_C$  and  $I_R$  represent the current of the grid, the load, the passive branch, the active branch and the FSRC branch, respectively.  $Z_S$ ,  $Z_F$  and  $Z_R$  represent the grid impedance, the PPF impedance and the FSRC impedance, respectively.  $U_F$  is the terminal voltage of the harmonic source.

The APF is controlled as a current source, where:

$$I_C = -I_{Lh} \quad (1)$$

If the harmonic voltage of the grid  $U_{Sh}$  is zero and only the harmonics generated by the nonlinear load are considered. The single-phase equivalent circuit about  $I_{Lh}$  of the RITHAF is shown in Fig.3.  $I_{Sh}$ ,  $I_{Fh}$  and  $I_{Rh}$  represent the harmonic current of the grid, the passive branch and the FSRC branch, respectively.  $Z_{Sh}$ ,  $Z_{Fh}$  and  $Z_{Rh}$  represent the harmonic impedance of the grid, the PPF branch and the FSRC branch, respectively.  $U_{Fh}$  is the terminal harmonic voltage of the harmonic source. The system equations are expressed as:

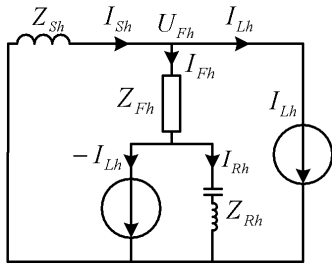


Fig. 3. Single-phase equivalent circuit about  $I_{Lh}$  of RITHAF.

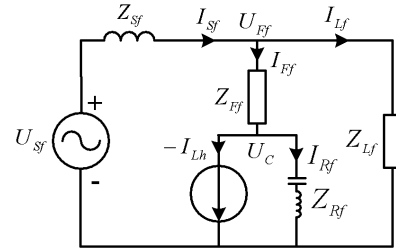


Fig. 5. Single-phase equivalent circuit about  $U_{Sf}$  of RITHAF.

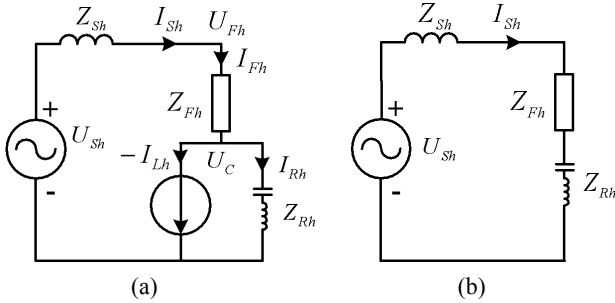


Fig. 4. Single-phase equivalent circuit about  $U_{Sh}$  of RITHAF. (a) Single-phase equivalent circuit of RITHAF when  $I_{Lh}$  is zero, (b) Equivalent circuit of fig.4 (a).

$$\begin{cases} I_{Sh} = I_{Fh} + I_{Lh} \\ U_{Fh} = -Z_{Sh}I_{Sh} \\ U_{Fh} = Z_{Fh}I_{Fh} + U_C \\ U_C = Z_{Rh}I_{Rh} \\ I_{Fh} = I_{Rh} + I_C \\ I_C = -I_{Lh} \end{cases} \quad (2)$$

where  $U_C$  is the voltage of the active part. According to (2),  $I_{Sh}$  and  $U_C$  can be expressed as:

$$I_{Sh} = \frac{Z_{Fh}}{Z_{Fh} + Z_{Sh} + Z_{Rh}} I_{Lh} \quad (3)$$

$$U_C = \frac{Z_{Fh}Z_{Rh}}{Z_{Fh} + Z_{Sh} + Z_{Rh}} I_{Lh} \quad (4)$$

According to Fig.3, the APF of the RITHAF is equivalent to the harmonic impedance, which is connected with the grid in series. The magnitude of  $Z_{Rh}$  is much higher than that of the harmonic impedance  $Z_{Fh}$ . Therefore, the harmonics generated by a nonlinear load will flow to the PPF. The harmonic current injected to the grid will be low, which is nearly zero.

Considering the compensation of the RITHAF to the harmonics voltage of the grid  $U_{Sh}$  and assuming that  $I_{Lh}$  is zero, the single-phase equivalent circuit is shown in Fig.4 (a). The system equations are expressed as:

$$\begin{cases} U_{Sh} = Z_{Sh}I_{Sh} + U_{Fh} \\ U_{Fh} = Z_{Fh}I_{Fh} + U_C \\ U_C = Z_{Rh}I_{Rh} \\ I_{Sh} = I_{Fh} \\ I_{Fh} = I_{Rh} + I_C \\ I_C = -I_{Lh} \\ I_{Lh} = 0 \end{cases} \quad (5)$$

According to (5),  $I_{Sh}$  and  $U_C$  can be rewritten as:

$$I_{Sh} = \frac{U_{Sh}}{Z_{Fh} + Z_{Sh} + Z_{Rh}} \quad (6)$$

$$U_C = \frac{Z_{Rh}}{Z_{Fh} + Z_{Sh} + Z_{Rh}} U_{Sh} \quad (7)$$

From (6), Fig4.(a) can be equivalent to the circuit shown in Fig4.(b). If  $|Z_{Rh}| \gg |Z_{Fh} + Z_{Sh}|$ , the harmonic currents generated by  $U_{Sh}$  do not flow into the PPF, and the PPF will not overload.

According to (3-4), (6-7) and the superposition theory, if  $Z_{Rh}$  is very large, the RITHAF has excellent properties in harmonic suppression.  $I_{Sh}$  and  $U_C$  can be expressed as:

$$\begin{cases} I_{Sh} = 0 \\ U_C = Z_{Fh}I_{Lh} + U_{Sh} \end{cases} \quad (8)$$

For the fundamental wave voltage of the grid  $U_{Sf}$ , a single-phase equivalent circuit is shown in Fig.5.  $U_{Ff}$  is the terminally fundamental wave voltage of the harmonic source.  $I_{Sf}$ ,  $I_{Lf}$ ,  $I_{Ff}$ , and  $I_{Rf}$  represent the fundamental wave current of the grid, the load, the passive branch and the FSRC branch, respectively.  $Z_{Sf}$ ,  $Z_{Ff}$  and  $Z_{Rf}$  represent the fundamental wave impedance of the grid, the PPF branch and the FSRC branch, respectively. The APF only receives harmonic currents. The fundamental wave current will not flow into the APF. Since the PPF must compensate the reactive power, there must be some fundamental wave reactive current  $I_{Ff}$  flowing into  $Z_{Ff}$ . The APF is controlled as a harmonic current source, which is equivalent to an open circuit for the fundamental wave current. The

fundamental wave impedance of the FSRC  $Z_{Rf}$  is nearly zero. Therefore, all of  $I_{Ff}$  flows into the FSRC. That is to say:

$$I_{Rf} = I_{Ff} \quad (9)$$

The fundamental wave voltage of the APF  $U_{Cf}$  is expressed as:

$$U_{Cf} = Z_{Rf} I_{Ff} \approx 0 \quad (10)$$

The APF does not bear the fundamental wave voltage or no fundamental wave current. Therefore, the fundamental wave capacity of the APF is zero in theory. The power grade of the switch devices is decreased significantly. As a result, the initial investment of the RITHAF is reduced.

The harmonic compensation ability of the RITHAF depends on the harmonic impedance  $Z_{Rh}$  of the FSRC branch for the  $n$ th harmonic.

$$Z_{Rh} = jn\omega_S L_R + \frac{1}{jn\omega_S C_R} = j \frac{n^2 - 1}{n\omega_S C_R} \quad (11)$$

where  $\omega_S$  is fundamental angular frequency,  $L_R$  and  $C_R$  are the inductor and capacitor of the FSRC branch, respectively. In (11), the inductor internal resistance of the FSRC is not considered. The smallest harmonic component is the second harmonic,  $n=2$ . The second harmonic impedance of the FSRC must be larger than the constant  $K_1$ , where:

$$\frac{2^2 - 1}{2 \times 2\pi \times 50 \times C_R} > K_1 \quad (12)$$

where:

$$C_R < \frac{3}{200\pi K_1} \quad (13)$$

The relationship between the second harmonic impedance  $Z_{R2}$  and the  $n$ th harmonic impedance  $Z_{Rn}$  is expressed as:

$$\frac{Z_{Rn}}{Z_{R2}} = \frac{2(n^2 - 1)}{3n} \quad (14)$$

Hence the third harmonic impedance is 16/9 times the second harmonic impedance. The fifth harmonic impedance is 48/15 times the second harmonic impedance.

### III. STUDY ON THE CONTROL STRATEGY OF THE RITHAF

The performance of the RITHAF is influenced by different control strategies. The different performances of the RITHAF will be obtained, when the RITHAF is controlled as a current source or as a voltage source, respectively. A suitable control strategy is chosen for the engineering application in this section.

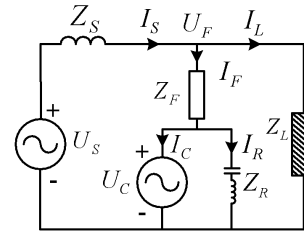


Fig. 6. Single-phase equivalent circuit of RITHAF.

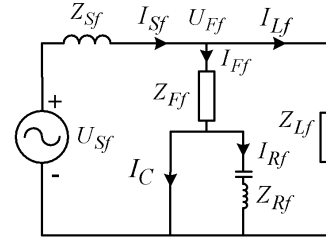


Fig. 7. Single-phase equivalent circuit about  $U_{Sf}$  of RITHAF.

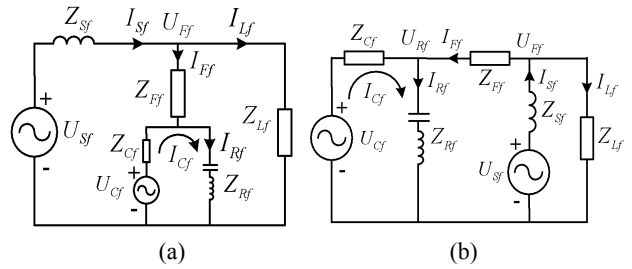


Fig. 8. Circuit of fundamental wave circulation. (a) Single-phase equivalent circuit of RITHAF in fundamental wave, (b) Equivalent circuit of fig.8 (a).

When the APF is controlled as a harmonic voltage source:

$$U_C = KI_{Sh} \quad (15)$$

where  $K$  is the controlled gain of  $I_{Sh}$ . If  $K$  is not too large, the fundamental wave current will flow into the APF. The capacity of the APF is increased.

If the active part of the RITHAF is considered as an ideal harmonic voltage source, it is equivalent to a short-circuit in the fundamental wave voltage  $U_{Sf}$ , as shown in Fig.7. The fundamental wave impedance of the FSRC  $Z_{Rf}$  is very small. However, all of the fundamental wave current through the PPF will be injected to the APF. However, the APF and the output filter as well as the coupling transformer show certain impedance. If their equivalent fundamental wave impedance  $Z_{Cf}$  is much larger than  $Z_{Rf}$ , the fundamental wave current will flow to the FSRC. In fact,  $Z_{Rf}$  is very small. Therefore,  $Z_{Cf}$  does not need to be too large.

There is another question about the fundamental wave circulation between the active part of the RITHAF and the FSRC branch. If the APF is considered as a controlled voltage source and its output voltage contains a small fundamental wave component. The equivalent circuit of the

RITHAF in the fundamental wave is shown in Fig.8 (a). As for  $U_{Cf}$ , the equivalent circuit is shown in Fig.8(b). Because  $Z_{Rf}$  is very small and nearly zero, the fundamental wave current of the APF  $I_{Cf}$  is expressed as:

$$I_{Cf} \approx \frac{U_{Cf}}{Z_{Cf} + Z_{Rf}} \approx \frac{U_{Cf}}{Z_{Cf}} \quad (16)$$

$U_{Cf}$  is much smaller than  $U_{Ff}$ , while it is not much smaller than  $Z_{Cf}$ . The simulation results are shown in Fig.9 under the condition that the APF is considered as a harmonic voltage source. In Fig.9,  $i_{Sa}$ ,  $i_{Fa}$ ,  $i_{Ca}$ ,  $i_{Ra}$  and  $V_{Ca}$  are the A phase current of the power grid, the PPF, the APF, the FSRC and the A phase fundamental wave voltage of the APF, respectively. The output-voltage error of the APF is very small in the simulation experiments. However, the fundamental wave component in  $i_{Ca}$  is very large from Fig.9. The fundamental wave component in the FSRC is larger than in the PPF. This shows that there is a fundamental wave circulation between the APF and the FSRC. The fundamental wave circulation will be bigger if the RITHAF is applied in higher voltage system.

$Z_{Cf}$  must be increased in order to decrease the fundamental wave current injected to the APF, which depends on the system voltage grade and the system control error. The equivalent impedance of the coupling transformer at the APF side shows inductive, and the fundamental wave impedance  $Z_{Cf}$  becomes larger as the harmonic impedance is increased, which will undoubtedly decrease the capability of the harmonic suppression of the RITHAF.

If the APF is controlled as a harmonic voltage source, there will be some contradiction between improving the properties of the harmonic suppression and reducing the fundamental wave current in the APF.

The APF does not bear the fundamental wave voltage or the fundamental wave current if the APF is considered as a harmonic current source whose capacity is very small. It is more economic relatively. In fact, in order to keep the DC voltage constant and to compensate the loss of the VSC and the DC-side capacitor, some small fundamental wave current will be injected to the APF. Or there is little fundamental wave current component  $I_{Cf}$  in the output current of the APF shown in Fig.10 (a).  $Z_{Rf}$  is connected with the other parts of the system in parallel. Because  $Z_{Rf}$  is very small,  $I_{Cf}$  will flow to the FSRC, as shown in Fig10. (b). The fundamental wave voltage of the APF is expressed as:

$$U_{Cf} = U_{Rf} \approx Z_{Rf} I_{Cf} \approx 0 \quad (17)$$

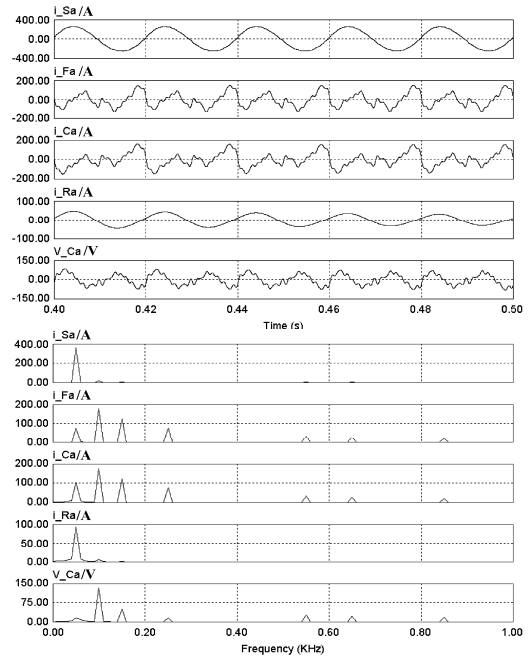


Fig. 9. Waveforms and spectrum of fundamental wave circulation.

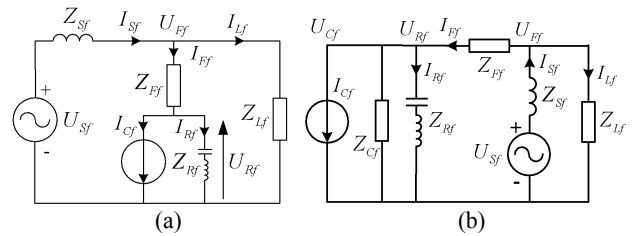


Fig. 10. Fundamental wave equivalent circuit while the existence of  $I_{Cf}$ . (a) Single-phase equivalent circuit of RITHAF when  $I_{Cf}$  is not zero, (b) Equivalent circuit of fig.10 (a).

where  $U_{Rf}$  is the fundamental wave voltage of the FSRC branch. The APF will not bear the fundamental wave voltage if the APF is considered as a harmonic current source no matter how much  $Z_{Cf}$  is. Therefore,  $Z_{Cf}$  and its harmonic impedance can be very small. The capacity of the APF will be decreased. Better performance and economy can be obtained to control the APF as a harmonic current source.

#### IV. CHARACTERISTIC ANALYSIS OF THE RITHAF

##### A. Influences of Power Grid Impedance Changes

The harmonic compensating characteristic of the PPF is influenced by the grid impedance  $Z_S$  greatly, but the APF can overcome the influence of  $Z_S$  well.

Firstly, two evaluation indexes are introduced

(1) The harmonic suppression functions of the harmonic source. This is defined as the ratio of the grid harmonic

current  $I_{Sh}$  and the harmonic current  $I_{Lh}$  of the harmonic source when  $U_{Sh}$  is zero. This represents the harmonic compensating ability of the filter. As for the PPF, the function is expressed as:

$$\left. \frac{I_{Sh}}{I_{Lh}} \right|_{U_{Sh}=0} = \frac{Z_{Fh}}{Z_{Fh} + Z_{Sh}} \quad (18)$$

As for the RITHAF, from (3), the function is expressed as:

$$\left. \frac{I_{Sh}}{I_{Lh}} \right|_{U_{Sh}=0} = \frac{Z_{Fh}}{Z_{Fh} + Z_{Sh} + Z_{Rh}} \quad (19)$$

(2) The harmonic suppression functions of the grid harmonic. This is defined as the ratio of  $I_{Sh}$  and  $U_{Sh}$  when  $I_{Lh}$  is zero.

As for the PPF, the function is expressed as:

$$\left. \frac{I_{Sh}}{U_{Sh}} \right|_{I_{Lh}=0} = \frac{1}{Z_{Fh} + Z_{Sh}} \quad (20)$$

As for the RITHAF, from (6), the function is expressed as:

$$\left. \frac{I_{Sh}}{U_{Sh}} \right|_{I_{Lh}=0} = \frac{1}{Z_{Fh} + Z_{Sh} + Z_{Rh}} \quad (21)$$

The harmonic impedance of the PPF is expressed as:

$$Z_{Fh} = \frac{1}{\frac{1}{R_2 + j\omega L_2 + \frac{1}{j\omega C_2}} + \frac{1}{R_3 + j\omega L_3 + \frac{1}{j\omega C_3}} + \frac{1}{R_5 + j\omega L_5 + \frac{1}{j\omega C_5}} + \frac{1}{\frac{1}{j\omega C_H} + \frac{j\omega L_H R_H}{R_H + j\omega L_H}}} \quad (22)$$

where  $\omega$  is the harmonic angular frequency;  $R_2, R_3, R_5$  and  $R_H$  stand for the filter inductor internal resistances of the 2<sup>nd</sup>, 3<sup>rd</sup>, 5<sup>th</sup> PPF and the High pass PPF, respectively;  $C_2, C_3, C_5$  and  $C_H$  stand for the filter capacitors of the 2<sup>nd</sup>, 3<sup>rd</sup>, 5<sup>th</sup> PPF and the High pass PPF, respectively;  $L_2, L_3, L_5$  and  $L_H$  stand for the filter inductors of the 2<sup>nd</sup>, 3<sup>rd</sup>, 5<sup>th</sup> PPF and the High pass PPF, respectively.

The harmonic impedance of the FSRC is expressed as:

$$Z_{Rh} = R_R + j\omega L_R + \frac{1}{j\omega C_R} \quad (23)$$

where  $R_R$  stand for the inductor internal resistance of the FSRC.

The harmonic impedance of the grid is expressed as:

$$Z_{Sh} = R_S + j\omega L_S \quad (24)$$

where  $R_S$  and  $L_S$  stand for the inductor internal resistance and inductor of the grid, respectively. The inductor internal resistances of the PPF and FSRC are obtained by the quality factor  $Q$ .

The influence of  $Z_{Sh}$  on the harmonic suppression functions of the harmonic source and the grid harmonic are shown in Fig.11 and Fig.12, respectively. In Fig.11 and Fig.

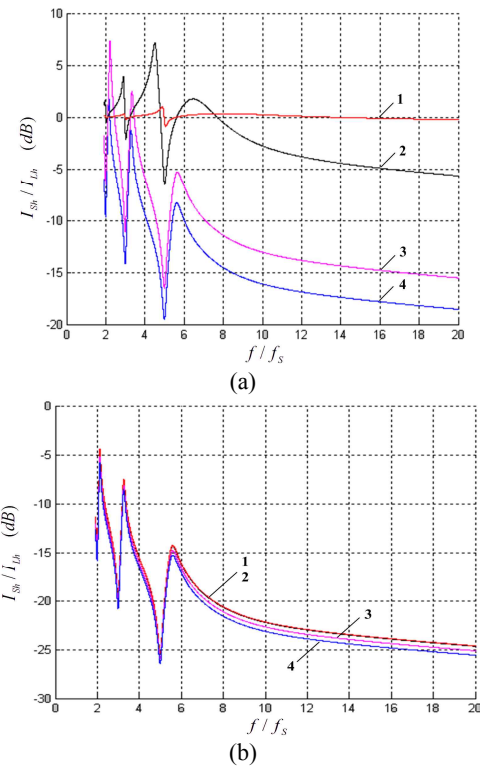


Fig. 11. Influence of  $Z_{Sh}$  on harmonic suppression functions of harmonic source. (a) Harmonic compensating characteristic of PPF by (18), (b) Harmonic compensating characteristic of RITHAF by (19).

12, the curves 1, 2, 3 and 4 stand for when the inductor of grid  $L_S$  is 0.05mH, 0.5mH, 5mH and 10mH, when  $R_S$  is 0.01  $\Omega$ , respectively. In Fig.11 and Fig.12, figures (a) and (b) stand for the harmonic compensating characteristic of the PPF and the RITHAF in different harmonic suppression functions, respectively. The unit of the harmonic suppression function is represented by dB. The abscissa is the ratio of harmonic frequency  $f$  and fundamental wave frequency  $f_s$ .

From Fig.11 (a) and Fig.12 (a), it can be seen that the harmonic suppression function is changed greatly if  $L_S$  has different values, regardless of the harmonic current of the harmonic source or the harmonic voltage of the grid. From Fig.11 (b) and Fig.12 (b), it can be seen that the grid impedance has little effect on the harmonic compensating characteristic of the RITHAF. The value of the harmonic suppression function is negative with all frequency even if  $L_S$  is very small.

Therefore, it can be concluded that the harmonic compensating characteristic of the PPF is influenced by the grid impedance. When the grid impedance is smaller, the harmonic suppression performance of the PPF is worse. When the grid impedance is bigger, the harmonic suppression

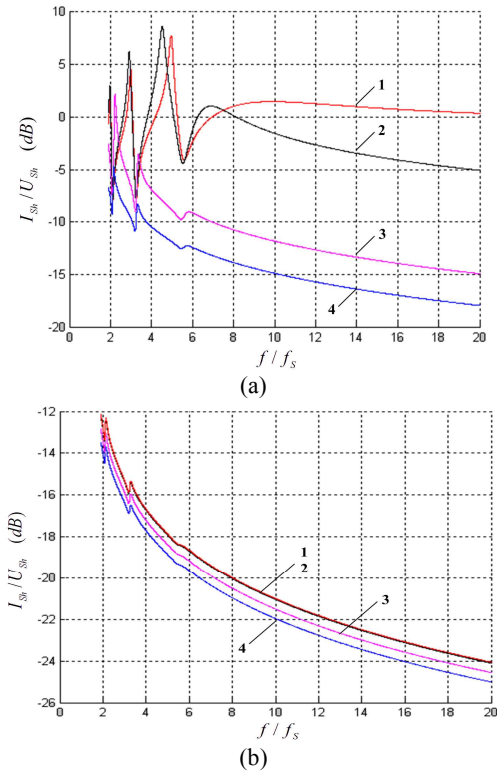


Fig. 12. Influence of  $Z_{sh}$  on harmonic suppression functions of grid harmonic. (a) Harmonic compensating characteristic of PPF by (20), (b) Harmonic compensating characteristic of RITHAF by (21).

performance of the PPF is better. The harmonic compensating characteristic of the RITHAF is basically not influenced by the grid impedance. When the grid impedance is bigger, the harmonic suppression performance of the RITHAF is also better. It has good compensating characteristic to the harmonics at all frequencies.

### B. Influences of Passive Power Filter Detuning on the Compensating Characteristics

The property of the PPF only influences the capacity of the APF, which does not influence the compensating characteristic of the RITHAF. If the tuned frequencies of the single tuned filters offset 10%, there will be two detuned situations. The first is that the tuned frequencies of the 2<sup>nd</sup>, 3<sup>rd</sup> and 5<sup>th</sup> PPF are 90Hz, 135Hz and 225Hz, respectively; the second is that the tuned frequencies are 110Hz, 165Hz and 275Hz, respectively. The influence of the PPF detuning on the harmonic suppression functions of the harmonic source and the grid harmonic are shown in Fig.13 and Fig.14, respectively. In Fig.13 and Fig.14, curve 1 represents the tuned frequencies offset -10%, curve 2 represents the tuned frequencies offset zero, and curve 3 represents the tuned frequencies offset +10%.

From Fig.13 (a), it can be seen that for the harmonic current generated by the harmonic source, the harmonic

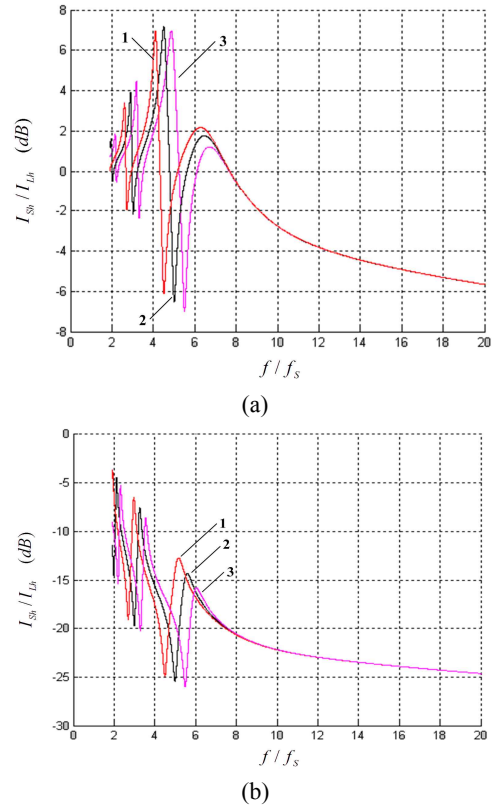


Fig. 13. Influence of PPF detuning on harmonic suppression functions of harmonic source. (a) Influence of PPF detuning on PPF in harmonic source, (b) Influence of PPF detuning on RITHAF in harmonic source.

compensating characteristic of the PPF will be very poor if the PPF is detuned (curve 1). Sometimes the harmonic is even amplified (curve 3). In Fig.13 (b), the harmonic compensating characteristic of the RITHAF is still good although the PPF is detuned. However, it is somewhat worse than with no PPF detuning. In Fig.14 (a), in terms of the grid harmonic, the harmonic compensating characteristic of the PPF will be poor if the PPF is detuned. The harmonic is even amplified. In Fig.14 (b), in terms of the grid harmonic, the three curves nearly coincide with each other, which shows that the harmonic compensating characteristic of the RITHAF is not influenced if the PPF is detuned.

Therefore, it can be concluded that the harmonic compensating characteristic of the PPF will be poor and even amplify the harmonic if the PPF is detuned. However, it has little effect on the RITHAF.

### C. Analysis of the DC-link Voltage

The FSRC branch in the RITHAF will bypass the fundamental wave current to decrease the APF power rating. However, this branch will make it difficult for the capacitor in the DC-link to get power from the grid through the inverter, which makes problems for the DC-link voltage control. A rectifier is used to provide voltage to the inverter in the paper.

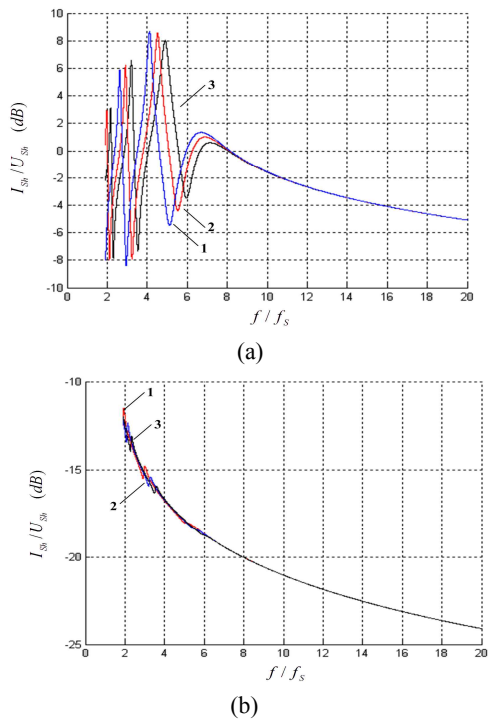


Fig. 14. Influence of PPF detuning on harmonic suppression functions of grid harmonic. (a) Influence of PPF detuning on PPF in grid harmonic, (b) Influence of PPF detuning on RITHAF in grid harmonic.

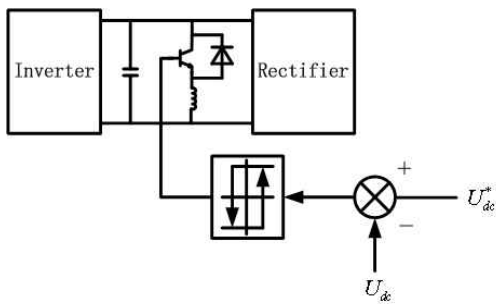


Fig. 15. Main topology of APF with release circuit.

However, there are reasons for the DC-link voltage to bring a serious ripple. 1) The large capacity of the reactive power between the grid and the APF. 2) The harmonic voltage on the FSRC from the grid is too high. The active power filter changing the power with the grid through the FSRC causes the DC-link ripple voltage. 3) The DC-link capacitor is charged because the voltage on the FSRC is too high when the grid voltage flickers.

The sharp rise in the DC-link voltage will easily damage the power switching equipment and the current flowing through the output filter will influence the safety of the system. In order to guarantee the performance and the safety of the inverter, the DC-link voltage should be kept balanced as long as a gateway is found to pour the active power into the grid. A pouring branch for the active power is added in

the inverter DC-link to keep the DC-link voltage stable [15]. The pouring branch of the active power added to the inverter DC-link is shown in Fig.15.

### V. SIMULATION RESULTS

Simulation results based on the RITHAF have been obtained using PSIM software. The system parameters are as follows: The three-phase line voltage is 10kV and its frequency is 50Hz. The harmonic source is a current source. It contains the fundamental wave current and the 2<sup>nd</sup>, 3<sup>rd</sup>, 5<sup>th</sup>, 11<sup>th</sup>, 13<sup>th</sup>, and 17<sup>th</sup> harmonic currents. The initial angles for each of the harmonics are zero,  $-2\pi/3$  and  $2\pi/3$  in A, B and C phase, respectively. The parameters of the PPF are shown in Table. I. Ideal harmonic current sources are applied in the simulation.

The current waveforms and frequency spectrums are shown in Fig.16.  $i_{La}$  represents the A phase current of the loads. The content of each harmonic current is shown in Table. II. The voltage waveforms and frequency spectrums of the grid  $V_{Fa}$  and the terminal voltage of the APF  $V_{Ca}$  are shown in Fig.17.

From the simulation results some conclusions can be drawn:

- (1) The proposed RITHAF has good performance in harmonic elimination. The simulation results show that the waveform  $i_{Sa}$  has a better sinusoidal characteristic and little harmonic contents.

TABLE I  
PARAMETERS OF RITHAF

	L	C	R	Q
2 <sup>nd</sup> PPF	33.65mH	75.28 uF		30
3 <sup>rd</sup> PPF	11.94 mH	94.29 uF		30
5 <sup>th</sup> PPF	3.72 mH	108.95 uF		32
High pass PPF	0.41 mH	374.5 uF	1 Ω	
FSRC	40.52mH	250 uF		35

TABLE II  
THE PEAK VALUE OF A PHASE (UNIT:A)

	fundamental	2 <sup>nd</sup>	3 <sup>rd</sup>	5 <sup>th</sup>	11 <sup>th</sup>	13 <sup>th</sup>	17 <sup>th</sup>
$i_{La}$	499.2	239.1	168.1	101.1	45.8	38.3	30.0
$i_{Sa}$	366.8	10.0	4.26	1.23	2.20	1.72	1.43
$i_{Fa}$	88.1	198.5	132.3	78.6	34.3	28.1	21.6
$i_{Ca}$	1.98	197.3	131.5	78.3	33.8	28.0	20.3
$i_{Ra}$	86.2	4.95	1.03	0.18	0.12	0.25	0.5

TABLE III  
Distortion of harmonics and the THD

	5 <sup>th</sup>	7 <sup>th</sup>	11 <sup>th</sup>	13 <sup>th</sup>	17 <sup>th</sup>	THD	PF
Before Compensated	19.0A	13.1A	7.4A	6.1A	4.0A	23%	0.84
After Compensated	0.8A	0.7A	1.0A	0.9A	0.9A	2.3%	0.93



(2) The proposed RITHAF can compensate some reactive power, because the waveform  $i_{Fa}$  has some fundamental wave current.

(3) The capacity of the APF is small. From table.2, it can be seen that the fundamental wave current  $i_{Ca}$  is very little. This is due to the fact that the APF of the RITHAF does not compensate reactive power and it only eliminates a part of the harmonics. From Fig.17, it can be seen that the fundamental wave voltage of the APF is only 29.4V. The APF does not need to endure the fundamental wave voltage and the fundamental wave current, so the total cost and capacity of APF can be noticeably decreased.

### VI. INDUSTRIAL APPLICATION RESULTS

There are many 6-pulse, 12-pulse, 24-pulse rectifiers and converters applied in the 10kV grid of a copper plant in the Anhui province of China, which result in a high harmonic current distortion and a low power factor. The proposed RITHAF system has been installed in the copper plant. An industrial platform was set up to prove the practicality of the proposed theory in this paper. A nonlinear load was connected to the 10kV power grid through a 8.5MVA transformer. The PPF are constructed with 5<sup>th</sup>, 7<sup>th</sup>, 11<sup>th</sup> PPF and high pass filters. Their capacities are 1400kVar, 1000kVar, 600kVar and 400kVar, respectively. The specifications of the inverter includes six pieces of PM400CLA120, six fast recovery diodes RM100HG-24S, and several non-inductance capacitors and resistors for the snubber circuit to reduce the turn-off surge voltage of the IGBT. A 16-bit fixed-point TMS320F28335 is used as a DSP controller. In addition, the A/D unit is composed of an MAX125 A/D converter. Data is sampled at equidistance during every grid cycle. The PWM waveforms are generated by a PWM unit of TMS320F28335. Fig.18 shows a prototype of the RITHAF system which consists of the PPF, the APF and the controller based on a DSP.

The load current waveform, the supply current waveform and their spectrums are shown in Fig.19. The distortion of the fifth, seventh, eleventh, thirteenth and seventeenth of the load current, the total harmonic distortion (THD) and the power factor (PF) are shown in Table. III both before and after compensation. The supply current waveform has already been approximated to a sinusoidal wave. Fig.19 (c) shows the output current waveform and spectrum of the APF. It can be seen that the APF only sustains harmonic current, which reduces the capacity of the APF. The application results have validated the practicality of the proposed RITHAF.

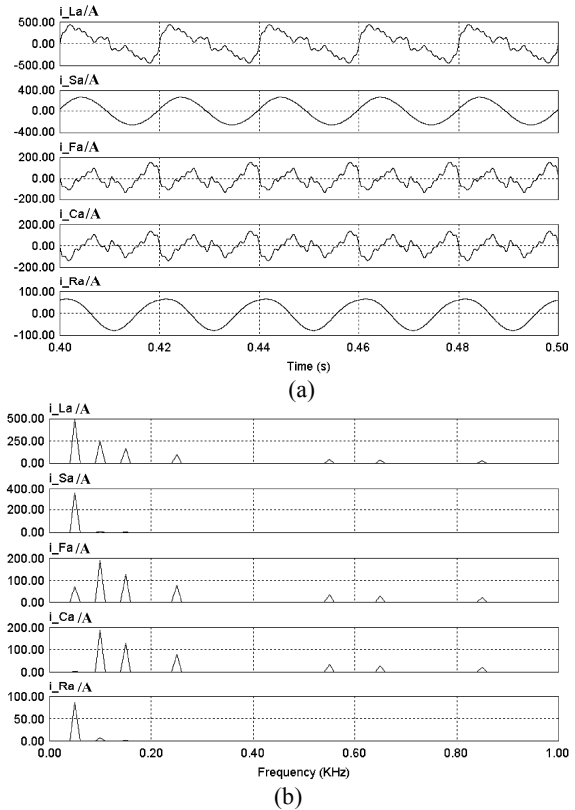


Fig. 16. Current waveforms and spectrums of A phase. (a) Current waveforms of A phase, (b) Current spectrums of A phase.

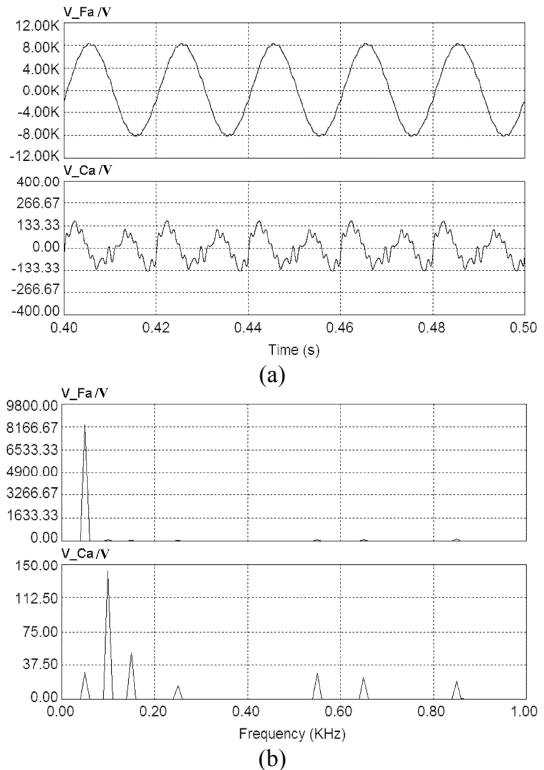


Fig. 17. Voltage waveforms and spectrums of  $V_{Fa}$  and  $V_{Ca}$ . (a) Waveforms of  $V_{Fa}$  and  $V_{Ca}$ , (b) Spectrums of  $V_{Fa}$  and  $V_{Ca}$ .

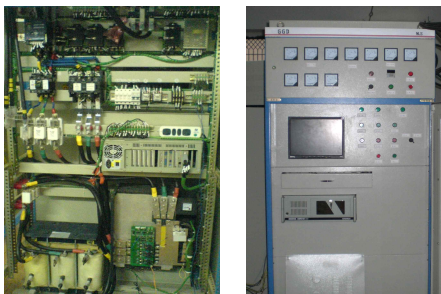
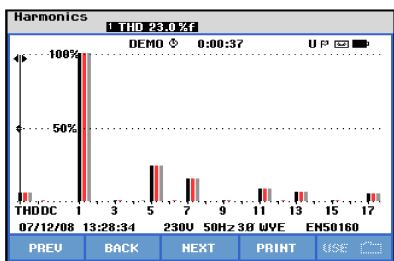
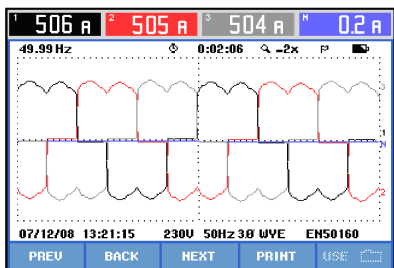
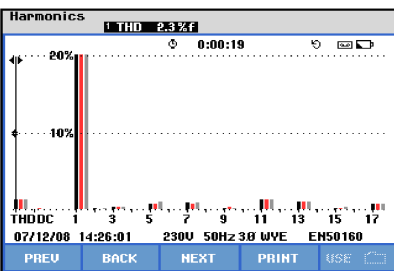
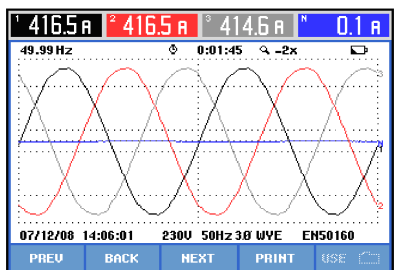


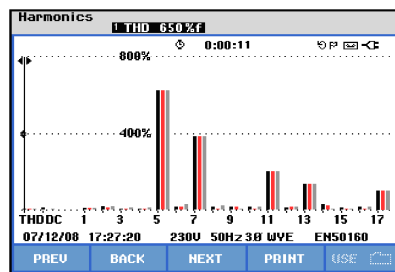
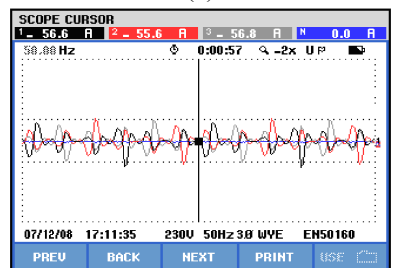
Fig.18. Prototype of the RITHAF system.



(a)



(b)



(c)

Fig. 19. Industrial application results. (a) Load current and spectrum before compensated, (b) Supply current and spectrum when the RITHAF is adopted, (c) Waveform and spectrum of APF output current.

VII. CONCLUSIONS

A kind of Resonant Impedance Type Hybrid Active Power Filter (RITHAF) is proposed in this paper. Its principle and control methods are discussed. It is more economical if the RITHAF is viewed as a current source. In addition, the influence of system parameters changes on the compensating performance of the RITHAF are also studied. Finally, simulation and industrial application results show that the RITHAF has excellent performance in harmonic suppression and reactive power compensation. The capacity of the active part and the power grade of the switch devices are low, which is suitable for medium and high voltage systems.

ACKNOWLEDGMENT

This work was supported by the National Basic Research Program of China (973 Program) (Project No.2009CB219706), The growth program of Hunan University for young teachers and The Scientific Research plan of Hunan Provincial Science and Technology Department of China(2012CK4017).

REFERENCES

- [1] Y. Han, "Control Strategies for Multilevel APFs Based on the Windowed-FFT and Resonant Controllers," *Journal of Power Electronics.*, Vol. 12, No. 3, pp. 509–517, May 2012.
- [2] Y. He, J. Liu, J. Tang, Z. Wang, and Y. Zou, "Theoretical Analysis and Control of DC Neutral-point Voltage Balance of Three-level Inverters in Active Power Filters," *Journal of Power Electronics.*, Vol. 12, No. 2, pp. 344–355, Mar. 2012.
- [3] F. Zhang and Y. Yan. "Selective harmonic elimination PWM control scheme on a three-phase four-leg voltage source inverter," *IEEE Trans. Power Electron.*, Vol. 24, No. 7, pp. 1682–1689, Jul. 2009.
- [4] P. Lohia, M. K. Mishra, K. Karthikeyan, and K. Vasudevan, "A minimally switched control algorithm for three-phase four-leg VSI topology to compensate unbalanced and nonlinear load," *IEEE Trans. Power Electron.*, Vol. 23, No. 4, pp. 1935–1944, Jul. 2008.

- [5] D. O. Abdeslam, P. Wira, J. Mercklé, D. Flieller, and Y.-A. Chapuis, "A unified artificial neural network architecture for active power filters," *IEEE Trans. Ind. Electron.*, Vol. 54, No. 1, pp. 61-76, Feb. 2007.
- [6] K. R. Uyyuru, M. K. Mishra, and A. Ghosh, "An optimization-based algorithm for shunt active filter under distorted supply voltages," *IEEE Trans. Power Electron.*, Vol. 24, No. 5, pp. 1223-1232, May 2009.
- [7] L. Asiminoaei, P. Rodriguez, and F. Blaabjerg, "Application of discontinuous PWM modulation in active power filters," *IEEE Trans. Power. Electron.*, Vol. 23, No.4, pp.1692-1706, Jul. 2008.
- [8] P. Salmerón and S. P. Litr'an, "A control strategy for hybrid power filter to compensate four-wires three-phase systems," *IEEE Trans. Power. Electron.*, Vol. 25, No. 7, pp.1923-1931, Jul. 2010.
- [9] Z. Wang, Q. Wang, W. Yao, and J. Liu, "A series active power filter adopting hybrid control approach," *IEEE Trans. Power Electron.*, Vol. 16, No. 3, pp. 301-310, May. 2001.
- [10] D. Li, Q. Chen, Z. Jia, and C. Zhang, "A high-power active filtering system with fundamental magnetic flux compensation," *IEEE Trans. Power Del.*, Vol. 21, No. 2, pp. 823-830, Apr. 2006.
- [11] V. F. Corasaniti, M. B. Barbieri, P. L. Arnera, and M. I. Valla, "Hybrid active filter for reactive and harmonics compensation in a distribution network," *IEEE Trans. Ind. Electron.*, Vol.56, No.3, pp. 670-677, Mar. 2009.
- [12] C. Zhang, Q. Chen, Y. Zhao, D. Li, and Y. Xiong, "A novel active power filter for high-voltage power distribution systems application," *IEEE Trans. Power Del.*, Vol. 22, No. 2, pp. 911-918, Apr. 2007.
- [13] A. Luo, Z. Shuai, W. Zhu, and Z. J. Shen, "Combined System for Harmonic Suppression and Reactive Power Compensation," *IEEE Trans. Ind. Electron.*, Vol.56, No.2, pp. 418-428, Feb. 2009.
- [14] A. Luo, C. Tang, Z. K. Shuai, W. Zhao, F. Rong, and K. Zhou, "A novel three-phase hybrid active power filter with a series resonance circuit tuned at the fundamental frequency," *IEEE Trans. Ind. Electron.*, Vol. 56, No.7, pp. 2341-2440, Jul. 2009.
- [15] A. Luo, Z. K. Shuai, Z. J. Shen, W. J. Zhu, and X. Y. Xu, "Design considerations for maintaining dc-side voltage of hybrid active power filter with injection circuit," *IEEE Trans. Power. Electronics.*, Vol. 24, No. 1, pp. 75-84, Jan. 2009.



**Lu Fang** was born in Hunan, China, in 1983. She received her B.S. and Ph.D. from the College of Electrical and Information Engineering, Hunan University, Changsha, China, in 2005 and 2011, respectively. Since 2011, she has been a Lecturer in the College of Electrical and Information Engineering, Hunan University. She is currently engaged in research on harmonics suppression, reactive power compensation, microgrid power quality, and electric power savings. She has published over 20 journal and conference articles.



**Xian-yong Xu** was born in Henan, China, in 1981. He received his B.S. and Ph.D. from the College of Electrical and Information Engineering, Hunan University, Changsha, China, in 2001 and 2005, respectively. Since 2010, he has been an Engineer with Hunan Electric Power Company Test and Research Institute, Changsha, China. He is currently engaged in research on harmonics suppression and reactive power compensation for power electronic devices and active power filters, microgrid power quality, UHV AC test systems and their application for UHV AC devices, and electric power savings. He has published over 20 journal and conference articles. He was a recipient of the 2007 Scientific and Technological Award from the National Mechanical Industry Association of China.



**An Luo** was born in Changsha, China, in 1957. He received his B.S. and M.S. from Hunan University, Changsha, China, in 1982 and 1986, respectively, and his Ph.D. from Zhejiang University, Zhejiang, China, in 1993. He was with the Central South University, as a Professor from 1996 to 2002. Since 2003, he has been a Professor at Hunan University. He is currently engaged in research on power conversion systems, harmonics suppression, reactive power compensation, and intelligent control theory and application. He has published over 100 journal and conference articles. He was a recipient of the 2006 National Scientific and Technological Award of China, the 2005 Scientific and Technological Award from the National Mechanical Industry Association of China, and the 2007 Scientific and Technological Award from the Hunan Province of China. He is currently serving as the Associate Board Chairperson of the Hunan Society of Electrical Engineering. He is also serving as the Chief of the Hunan Electric Science and Application Laboratory.



**Yan Li** was born in Guangxi, China, in 1976. She received her B.S. and Ph.D. from the Central South University, Changsha, China, in 1999 and 2007, respectively. Since 2009, she has been a Lecturer in the School of Information Science and Engineering, Central South University. She is currently engaged in research on power conversion systems, harmonics suppression, reactive power compensation, and electric power savings.



**Chun-ming Tu** was born in Jiangxi, in 1976. He received his M.S. and Ph.D. from the Central South University, Changsha, China, in 2001 and 2004, respectively. He is currently engaged in research on electric power savings and active power filters.



**Hou-hui Fang** was born in Changsha, China, in 1956. He received his B.S. and M.S. from Hunan University, Changsha, China, in 1977 and 1991, respectively. Since 2005, he has been a Professor with the College of Electrical and Information Engineering, Hunan University. He is currently engaged in research on building electrical, power conversion systems, harmonics suppression, reactive power compensation, and electric power savings. He has published over 30 journal and conference articles. Since 2007, he has served as the Associate Chairperson of the Electrical Research Society in Hunan Colleges and Universities. From 2003 to 2007, he served as the Director of the Electrical Research Society in Chinese Colleges and Universities. He was a recipient of the 2005 Scientific and Technological Award from the National Mechanical Industry Association of China and the 2005 Scientific and Technological Award from the Hunan Province of China.